

Spin-spiral structure in ZnCr_2Se_4 across the whole field-temperature phase diagram

A. S. Cameron¹, Y. V. Tymoshenko¹, P. Y. Portnichenko¹, J. Gavilano², V. Tsurkan³, and D. S. Inosov¹

¹Institut für Festkörperphysik, TU Dresden, Helmholtzstraße 10, D-01069 Dresden, Germany

²Paul Scherrer Institut, CH-5232 Villigen PSI, Switzerland

³University of Augsburg, 86135 Augsburg, Germany

Material properties

- Magnetically frustrated spinel.
- Magnetic Cr^{3+} ions.
- Incommensurate spin spiral order.
- Curie temperature: $T_C = 21 \text{ K}$.
- Propagation vector: $k_h = 0.28 \text{ \AA}^{-1}$.
- Helical pitch: $\lambda_h = 22.4 \text{ \AA}$.

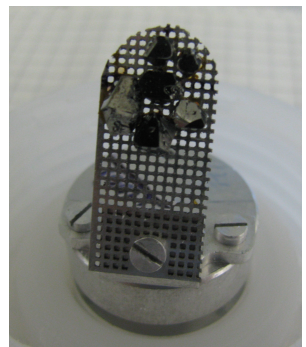


Fig. 1. Co-aligned single crystal mosaic of ZnCr_2Se_4 .

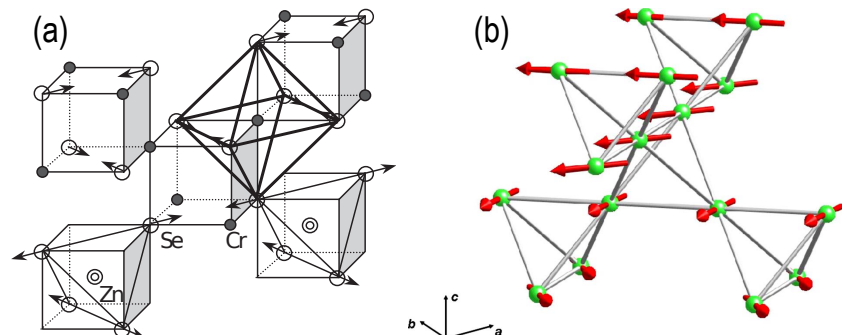
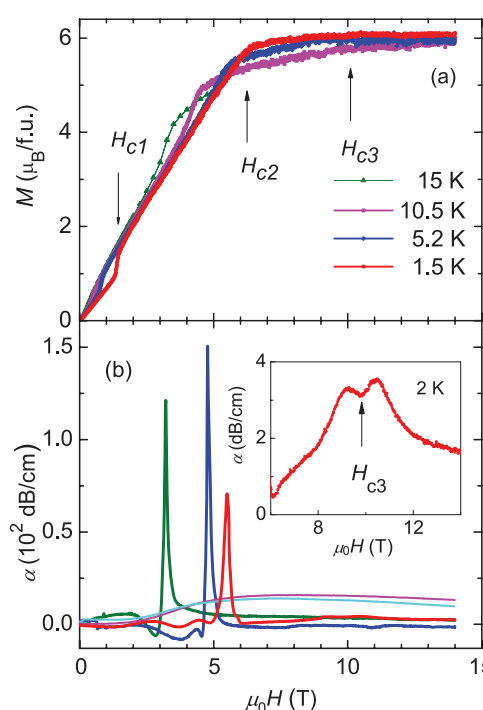


Fig. 2. (a) Spinel structure of ZnCr_2Se_4 [1]. Arrows indicate displacements of Se^{2-} ions in the orthorhombic phase below about 21 K (T_C). (b) Schematic representation of the magnetic structure of ZnCr_2Se_4 (only the Cr atoms displayed) [4].

Motivation



Sound velocity and magnetization measurements (Fig. 3) indicate the presence of a high-field phase between 6 and 10 T (green color in Fig. 8). It has been attributed to a “spin-nematic” phase [3], yet its true microscopic nature has not been understood. This motivated us to perform SANS measurements to check if long-range magnetic order is present in this phase.

Fig. 3. (a) Relative change of the attenuation α vs magnetic field at different temperatures in ZnCr_2Se_4 . (b) Magnetization curves at different temperatures for ZnCr_2Se_4 measured along the $\langle 001 \rangle$ axis [3].

- [1] M. Hidaka *et al.*, phys. stat. sol. (b) **236**, 9 (2003).
[2] A. Cameron, PhD thesis, University of Birmingham (2013).
[3] V. Felea *et al.*, Phys. Rev. B **86**, 104420 (2012).
[4] F. Yokaichiya *et al.*, Phys. Rev. B **79**, 064423 (2009).

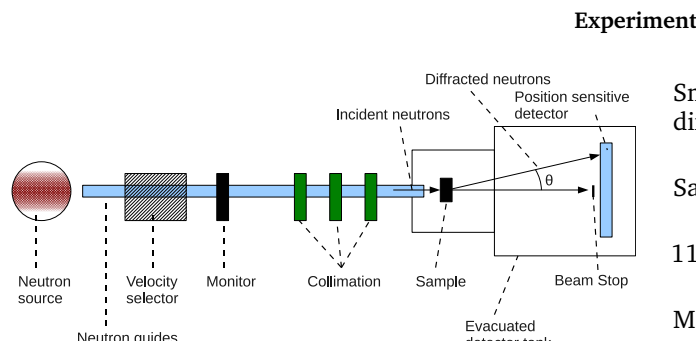


Fig. 4. Schematic of a SANS instrument [2].

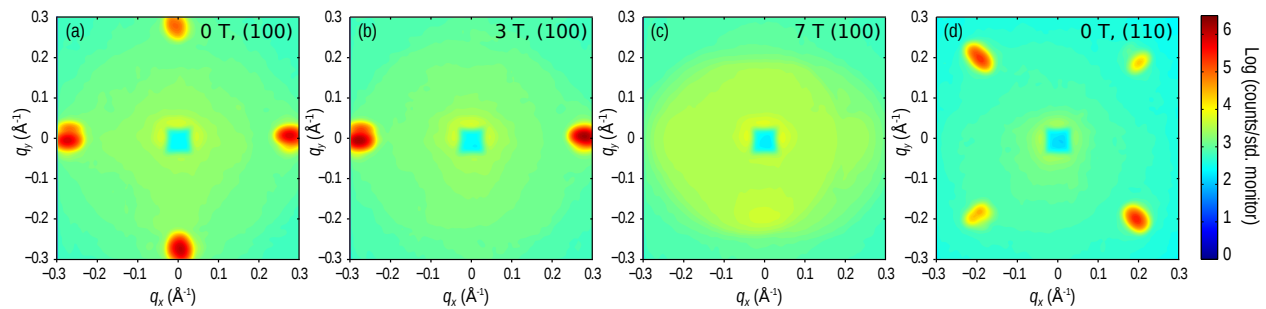


Fig. 5. Magnetic-field dependence of the low-temperature magnetic neutron diffraction patterns in ZnCr_2Se_4 . Typical neutron diffraction patterns are shown from each of the distinct phases and orientations observed during the experiment. The data demonstrate two phase transitions across B_{C1} and B_{C2} which are shown in phase diagram (Fig. 8).

Data analysis

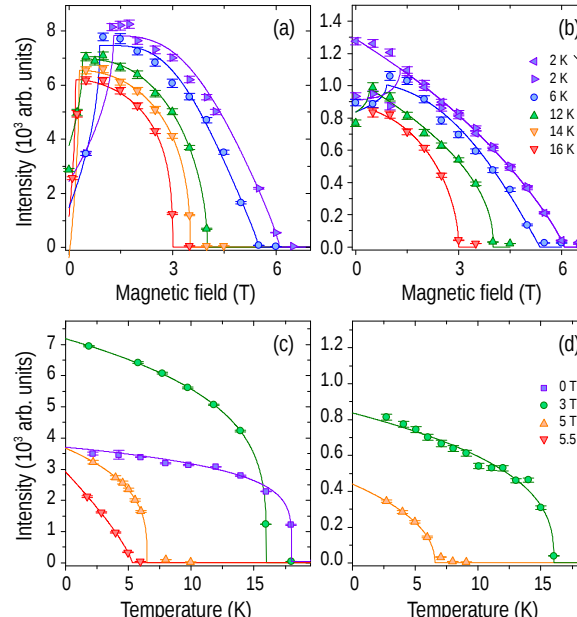


Fig. 6. Magnetic-field and temperature dependence of the magnetic Bragg intensity in ZnCr_2Se_4 , obtained by fitting the neutron-diffraction data.

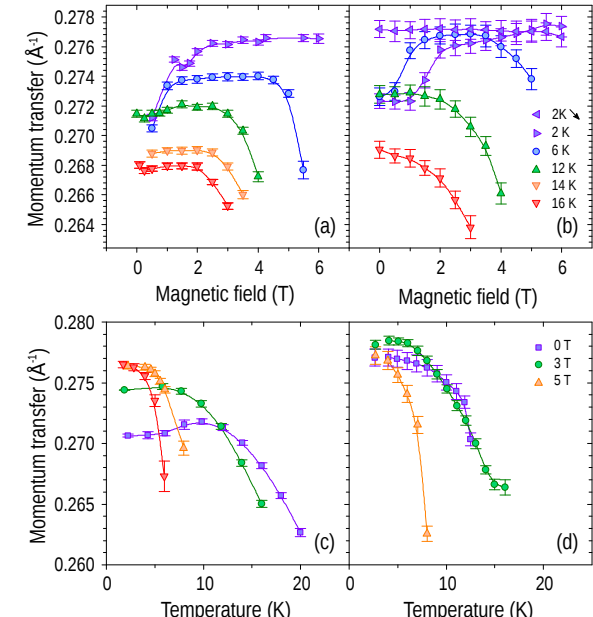


Fig. 7. Magnetic-field and temperature dependence of the magnetic propagation vector in ZnCr_2Se_4 , obtained by fitting the neutron-diffraction data.

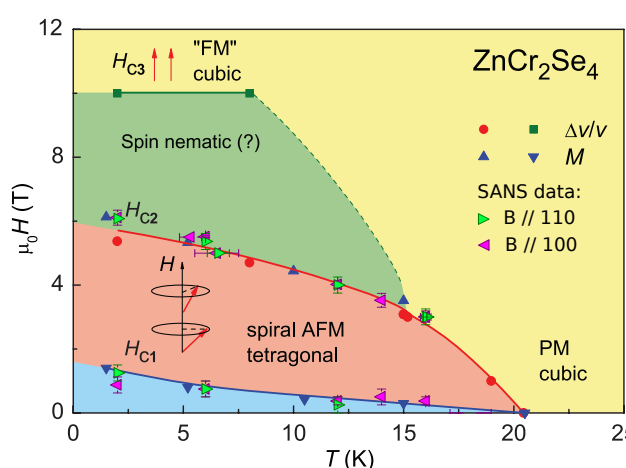


Fig. 8. Phase diagram of ZnCr_2Se_4 from a combination of ultrasound and magnetization measurements, reproduced from Ref. [3], onto which we have superimposed transition points from our SANS data.

Conclusions

- Magnetic Bragg peaks corresponding to long-range helical order are found below H_{C2} .
- The field H_{C1} corresponds to domain selection between different directions of the spin spiral.
- No anisotropy of H_{C1} or H_{C2} was observed for the two measured field directions.
- No incommensurate magnetic peaks were seen in the high-field (“spin-nematic”) phase.
- We observed a weak dependence of the propagation vector (helical pitch) on magnetic field and temperature that does not exceed 5%.